Comparative Study of C-H Stretch and Bend Vibrations in Methane Activation on Ni(100) and Ni(111)

L. B. F. Juurlink
Leiden Institute of Chemistry, Gorlaeus Laboratories, Leiden University, 2300 RA Leiden, The Netherlands

R. R. Smith, D. R. Killelea, and A. L. Utz
Department of Chemistry and W. M. Keck Foundation Laboratory, Tufts University, Medford, Massachusetts 02155, USA
(Received 2 December 2004; published 25 May 2005)

State-resolved measurements on clean Ni(100) and Ni(111) surfaces quantify the reactivity of CH_4 excited to $v = 3$ of the ν_4 bend vibration. A comparison with prior data reveals that $3\nu_4$ is significantly less effective than the ν_3 C-H stretch at promoting dissociative chemisorption, even though $3\nu_4$ contains 30% more energy. These results contradict statistical theories of gas-surface reactivity, provide clear evidence for vibrational mode specificity in a gas-surface reaction, and point to a central role for C-H stretching motion along the reaction path to dissociative chemisorption.

DOI: 10.1103/PhysRevLett.94.208303 PACS numbers: 82.20.Bc, 68.35.Ja, 68.49.Df, 82.65.+r

Vibrationally excited molecules can play a central role in gas-phase reactions, and recent state-resolved studies are revealing that these energized molecules may play a similarly important role in gas-surface reactivity [1–4]. Despite their importance in reactive environments, key questions regarding their dissociative chemisorption dynamics remain [5]. Here, we use an experimental approach that quantifies the reaction probability, S_0, of molecules in select vibrational states. We compare S_0 for CH_4 molecules containing two distinct types of vibrational excitation—an antisymmetric C-H stretch ($S_0^{\nu_3}$) and three quanta of the triply degenerate bending vibration ($S_0^{3\nu_4}$). Our data reveal that the more energetic $3\nu_4$ state is less reactive than ν_3 on both Ni(100) and Ni(111). These results offer the first direct comparison of C-H stretch and bend excitation in promoting CH_4 dissociation on a metal, establish the relative importance of C-H stretching and bending motion in promoting transition state access in this prototypical gas-surface reaction, and provide further evidence for nonstatistical, mode selective behavior in dissociative chemisorption on metal surfaces.

Methane dissociation on nickel is highly activated [6]. S_0 increases exponentially as translational energy (E_{trans}) and average vibrational energy (E_{vib}) increase [4,7,8]. Empirical and *ab initio* potential energy surfaces have a ''late'' barrier for dissociation [9–11]. Transition state calculations predict a significantly elongated active C-H bond that is bent relative to the C_3 axis of the nonreactive methyl group [12]. These findings point to important roles for both E_{trans} and E_{vib} in CH_4 activation.

The nature of methane's vibrational activation has been debated for many years. Early beam-surface scattering experiments established the importance of E_{vib} [7], but it has remained unclear which of methane's many vibrational modes were responsible for the activation—or whether all modes contributed equally. Collision induced dissociation measurements on Ni(111) suggested a key role for bending vibrations [13], but reduced dimensionality transition state calculations pointed to the importance of C-H stretching motion in accessing the transition state [9]. An empirical model that attributed all vibrational activation to a pseudodiatomic C-H oscillator successfully reproduced both beam and bulb measurements of CH_4 dissociation on Ni(100) [10]. Wave-packet calculations predicted vibrational-state-dependent differences in the coupling of E_{vib} to the surface [14]. The authors postulated that this effect could lead to mode specific reactivity, with C-H stretching states being most reactive. In contrast, a statistical model based on microcanonical unimolecular rate theory assumed equal reactivity on a per-energy basis for all CH_4 vibrational states and has successfully reproduced much of the experimental data for dissociation on Ni [15] and Pt [16] surfaces. Controversy persists because S_0 values averaged over the many vibrational states present in a typical CH_4 sample can obscure key details of the system's dynamical behavior.

This Letter describes experiments that quantify $S_0^{3\nu_4}$. The molecules impinge on clean Ni(100) or Ni(111) surfaces along the surface normal. High-level anharmonic force field calculations indicate that the $3\nu_4$ eigenstate we excite with our laser is nearly identical to a zero-order bending normal mode and that the laser-prepared ν_3 eigenstate is nearly identical to a zero-order C-H stretch normal mode state [17]. We can therefore compare S_0 for $3\nu_4$ with previously published data for ν_3 [4,18] to understand how C-H stretch and bend excitation promote CH_4 dissociation on low-index Ni surfaces.

We performed the experiments in a triply differentially pumped supersonic molecular beam-surface scattering apparatus [19]. A 2% mixture of CH_4 in H_2 expanded continuously from a 294, 400, 500, 550, or 600 K nozzle and formed the molecular beam. Infrared (IR) light from a

continuous wave, single mode laser intersected the molecular beam and excited a fraction of the molecules to $J = 2$ of the F_2 symmetry $3\nu_4$ vibration via the R(1) transition at 3876.7771 cm^{-1}. A room temperature pyroelectric detector translated into the molecular beam quantified IR absorption. Methane's long IR radiative lifetime and collision-free conditions in the beam ensured that the optically excited molecules impinged on the 475 K Ni surface in their initially prepared state. Auger electron spectroscopy (AES) quantified carbon deposition as a signature of dissociative chemisorption. We performed all measurements in the limit of low coverage (less than 0.12 ML C) and computed S_0 as the quotient of carbon's areal density on the surface (as determined by AES) and the integrated incident flux of CH_4.

We have shown [4] that Eq. (1) yields the reaction probability for the laser-excited state $S_0^{3\nu_4}$:

$$S_0^{3\nu_4} = \frac{S_0^{\text{LaserOn}} - S_0^{\text{LaserOff}}}{f_{\text{exc}}} + S_0^{v=0}. \quad (1)$$

We measured S_0 for CH_4 in the molecular beam with and without laser excitation (S_0^{LaserOn} and S_0^{LaserOff}, respectively) and quantified the fraction of molecules optically excited (f_{exc}) to calculate $S_0^{3\nu_4}$. At the energies studied here, $S_0^{v=0}$ contributes negligibly to $S_0^{3\nu_4}$.

Saturation measurements determined f_{exc} in our studies of ν_3 [19], but the weak $3\nu_4$ overtone transition precluded that approach here. Instead, we compared IR absorption signals for $3\nu_4$ and ν_3 excitation and found $f_{\text{exc}} = 0.0024$ for the $3\nu_4$ experiments on Ni(100). Experimental improvements prior to the Ni(111) work increased f_{exc} to 0.010–0.017, depending on molecular beam conditions. We independently validated our experimental measurements of f_{exc} by using instrument parameters determined in our ν_3 experiments, known Einstein coefficients for the ν_3 and $3\nu_4$ transitions [20], and measured IR radiation densities to calculate f_{exc}.

When f_{exc} is small, S_0^{LaserOn} and S_0^{LaserOff} differ little. To best quantify $S_0^{\text{LaserOn}} - S_0^{\text{LaserOff}}$, we rely on the localized deposition of laser-excited molecules on the Ni surface [21]. Figure 1 shows that molecules traveling toward the crystal edge have a transverse velocity component along the laser's propagation direction. When the laser is tuned to the center of the Doppler profile, it excites only molecules whose homogeneous linewidth overlaps with the laser's emission—i.e., those molecules traveling toward the crystal center. Molecules traveling toward the crystal edge are Doppler detuned from the laser's emission and are not excited. Spatially resolved AES measurements quantify C coverage at a series of points across the surface and allow us to measure S_0^{LaserOn} (center) and S_0^{LaserOff} (near edge) in a single experiment.

Carbon deposition maps from our prior studies of laser-excited CH_4 (ν_3) incident on Ni(100) with $E_{\text{trans}} = 50$ kJ/mol appear in Fig. 2(a). In the absence of laser excitation, the uniform CH_4 flux in the beam results in constant C coverage across the crystal (open symbols). With laser excitation (solid symbols) C deposition is enhanced near the crystal center. The measured quantities and Eq. (1) yield $S_0^{\nu_3} = 1.8 \times 10^{-3}$.

Figure 2(b) shows carbon deposition maps for CH_4 ($3\nu_4$) incident on a clean, 475 K Ni(100) surface with $E_{\text{trans}} = 50$ kJ/mol. Both the ν_3 and $3\nu_4$ experiments exposed each surface Ni atom to an incident flux of 26 laser-excited molecules, but the small f_{exc} for $3\nu_4$ required us to increase

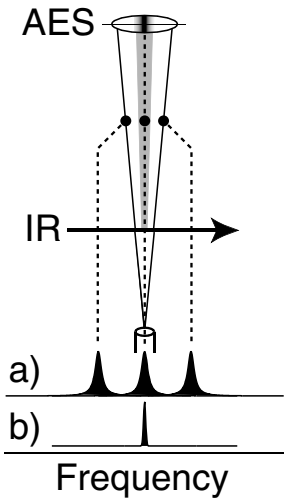

FIG. 1. Spatially localized deposition of laser-excited molecules. Molecules approach the surface in a diverging molecular beam. (a) Doppler-detuned absorption profiles for three paths. Molecules in center path absorb IR light (b) and show enhanced reactivity near the crystal center. AES spectra collected along the line shown generate data for Fig. 2.

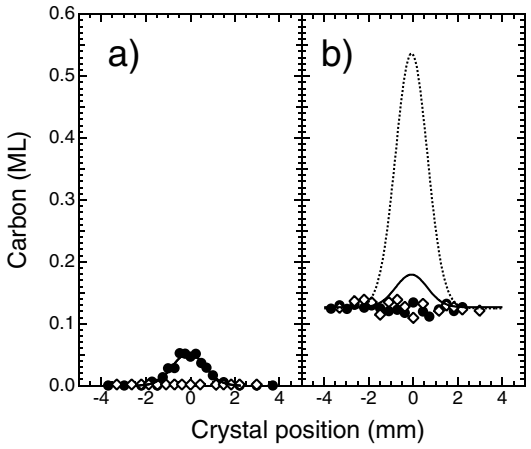

FIG. 2. Carbon deposition maps for CH_4 on Ni(100). (a) ν_3 excitation. Laser-excited molecules near the beam center are much more reactive than the Doppler-detuned molecules. (b) The $3\nu_4$ excitation. Solid line is expected deposition profile if $3\nu_4$ and ν_3 are equally reactive. Dashed line is expected deposition profile if $\eta_{\text{vib}}^{3\nu_4}$ and $\eta_{\text{vib}}^{\nu_3}$ are equal.

the dose time from 8 to 240 min, thereby increasing laser-off deposition 30-fold. Inspection of the $3\nu_4$ data reveals no detectable laser-enhanced deposition near the crystal center. Were $S_0^{\nu_3}$ and $S_0^{3\nu_4}$ equal, we would expect the carbon deposition map indicated by the solid line in Fig. 2(b). In fact, because $3\nu_4$ is more energetic than ν_3, statistical theories would predict $S_0^{3\nu_4}$ to be significantly greater than $S_0^{\nu_3}$. The dashed line in Fig. 2(b) shows the expected carbon deposition map if ν_3 and $3\nu_4$ were equally reactive on a per-energy basis. We conclude that at $E_{\text{trans}} = 50$ kJ/mol, $S_0^{3\nu_4} \leq 5 \times 10^{-4}$—at least 4 times less reactive than ν_3. Measurements at $E_{\text{trans}} = 9.9$ kJ/mol also failed to detect laser-enhanced reactivity.

We next studied the reactivity of CH_4 ($3\nu_4$) incident on Ni(111) and were able to quantify $S_0^{3\nu_4}$ over a wide range of E_{trans}, as shown in Fig. 3. Our ability to quantify $S_0^{3\nu_4}$ on Ni(111) but not on Ni(100) is consistent with prior work in which we found vibrational activation by ν_3 to be more pronounced on Ni(111) [18] than on Ni(100) [4]. Each point in Fig. 3 represents the average of at least three individual experiments. The vanishing difference between S_0^{LaserOn} and S_0^{LaserOff} prevented us from extending the E_{trans} range of the data beyond that shown. Experimental data and curves for $S_0^{\nu_3}$ and $S_0^{v=0}$ from a previous report appear for comparison [18]. Measurements of S_0^{LaserOff} (open circles) are upper limits on $S_0^{v=0}$. The curve passing near S_0^{LaserOff} represents our best estimate of $S_0^{v=0}$ [18]. On Ni(111), $3\nu_4$ molecules are up to 60-fold more reactive than those in $v = 0$ and about half as reactive as ν_3 molecules at all E_{trans} investigated.

Close examination of the S_0 curves in Fig. 3 allows us to compare how E_{trans} and E_{vib} in ν_3 and $3\nu_4$ activate CH_4 dissociation. Our experiments select the internal quantum state of the incident CH_4 molecules, their speed and direction of travel. Other important dynamical variables, including the surface impact site, the relative phase of the CH_4 vibration upon impact, the phase and amplitude of surface phonons, and the orientation of the active C-H bond, influence reaction energetics but lie beyond experimental control. The ensemble of CH_4 molecules incident on the surface samples a wide range of these dynamical variables, which leads to a distribution of E_{trans} thresholds for reaction [22]. S_0 measured at a particular E_{trans} reveals the fraction of the ensemble whose reaction threshold is $\leq E_{\text{trans}}$. Plots of S_0 vs E_{trans} in Fig. 3 are cumulative integrals of the effective reactive barrier height distribution along the E_{trans} coordinate. If E_{vib} reduces the need for E_{trans} by a constant amount without altering the shape of the distribution, then different vibrational states will have S_0 curves with an identical shape, but varying offset along the E_{trans} axis. The ratio of E_{vib} to the E_{trans} offset is η_{vib}, a measure of vibrational efficacy that is grounded in the system's energetics and applicable at all E_{trans} and S_0.

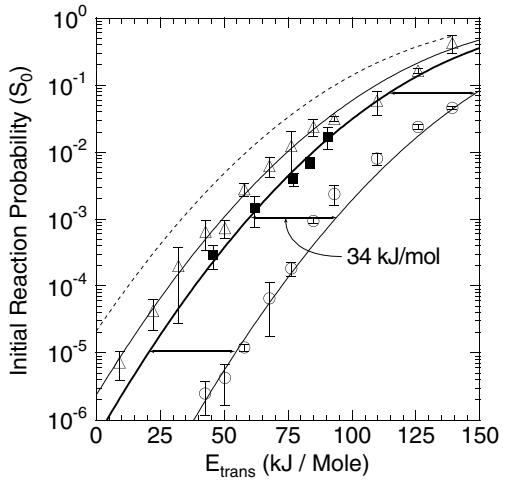

FIG. 3. State-resolved S_0 for CH_4 molecules incident on Ni(111) in $v = 0$ (circles), ν_3 (triangles), and $3\nu_4$ (squares). Arrows indicate the shift in $S_0^{3\nu_4}$ relative to $S_0^{v=0}$. The dashed line denotes the $S_0^{3\nu_4}$ curve expected if $\eta_{\text{vib}}^{3\nu_4}$ equaled $\eta_{\text{vib}}^{\nu_3}$.

Since the $S_0^{3\nu_4}$, $S_0^{\nu_3}$, and $S_0^{v=0}$ curves in Fig. 3 have comparable shapes, shifts of the curves along the E_{trans} axis reveal how ν_3 and $3\nu_4$ reduce the E_{trans} requirement for reaction. The $3\nu_4$ state contains 47 kJ/mol of E_{vib} and shifts $S_0^{3\nu_4}$ by 34 kJ/mol relative to $S_0^{v=0}$, leading to $\eta_{\text{vib}}^{3\nu_4} = 0.72$. This efficacy is significant and comparable to previously reported values for D_2 dissociation on copper [23] and CH_4 ($2\nu_3$) on Ni(100) [24], but is only about 60% of the $\eta_{\text{vib}}^{\nu_3} = 1.25$ reported for CH_4 dissociation on Ni(111) [18]. On Ni(100), a similar analysis using our upper limit on $S_0^{3\nu_4}$ indicates that $\eta_{\text{vib}}^{3\nu_4} < 0.5$ compared to $\eta_{\text{vib}}^{\nu_3} = 1.0$ on this surface. Therefore ν_3 is more effective than $3\nu_4$ in promoting methane dissociation on both Ni(111) and Ni(100), despite the fact that $3\nu_4$ contains nearly 30% more E_{vib}. The vibrational efficacy for both states is lower on Ni(100) than it is on Ni(111).

The data in Figs. 2 and 3 provide direct evidence for vibrational mode specificity in this gas-surface reaction. In contrast to predictions of statistical theories, which presuppose rapid and full redistribution of energy in the reaction complex, we observe a less energetic mode to be more reactive. This suggests that energy flow during reaction is uniquely influenced by the initial vibrational state of the gas-phase CH_4 molecule. Such behavior has a precedent in CH_4 dissociation on Ni. Beck *et al.* studied CH_2D_2 dissociation on Ni(100), and reported that two C-H stretch quanta in a localized C-H bond mode were 5 times more reactive than a more energetic state whose quanta were shared among the C-H bonds [25]. Our comparison of E_{vib} and E_{trans} in CH_4 (ν_3) activation on Ni(111) revealed nonstatistical behavior too [18].

We suggest three possible origins for the nonstatistical behavior we observe. First, ν_3 may better couple to the reaction coordinate. Such behavior is consistent with dynamical predictions of the "Polanyi rules" when applied to a gas-surface potential energy surface with many vibra-

tional coordinates [26]. Second, ν_3 and $3\nu_4$ may differ in their coupling to the substrate. Energy transfer propensity rules for E_{vib} predict more facile quenching of small (i.e., ν_4) quanta by low-frequency surface phonons. Such energy loss channels compete with reactive channels for available E_{vib}. Finally, state-resolved studies of D_2 on Cu [23] and CH_4 on Ni(100) [4,24]) show that η_{vib} for overtone states are less than that of the vibrational fundamental. Further study may reveal that η_{vib} for $\upsilon = 1$ of ν_4 exceeds $\eta_{vib}^{3\nu_4}$.

Our results impact the comparison of CH_4 dissociation data from beam and bulb experiments. Stretch quanta in CH_4 contain nearly twice the energy of C-H bend quanta, so CH_4 vibrations group into polyads of energetically similar states. Within each polyad, bending states are least energetic, and stretching states most energetic. High collision numbers in a bulb ensure thermal population of all vibrations, but vibrational cooling in a molecular beam is limited and produces a highly nonthermal vibrational state distribution [27]. The dominant V-T energy transfer channels in a beam favor small ΔE_{vib}, which serves to transfer population within each polyad to the lowest energy, or bending states [27]. The results presented here suggest that bending states may be significantly less reactive than C-H stretching states in the same polyad. Therefore, S_0 measurements made with the vibrational state distribution present in a supersonic molecular beam of CH_4 are biased toward the reactivity of bending states and likely underestimate the reactivity of a thermal vibrational state distribution, especially at low E_{trans} where S_0 varies most between excited vibrational states.

These data deepen our understanding of vibrational activation in CH_4 dissociation. First, both C-H stretching and bending vibrations contribute significantly to reactivity. Reduced dimensionality models that attribute all vibrational activation to C-H stretching states either will miss a significant source of reactivity present in a thermal sample or will severely overestimate the reactivity of C-H stretching states. Second, we find that $\eta_{vib}^{\nu_3}$ significantly exceeds $\eta_{vib}^{3\nu_4}$ for CH_4 dissociative chemisorption on Ni(100) and Ni(111) suggesting that the ν_3 antisymmetric C-H stretch coordinate is more effective than a C-H bending state ($3\nu_4$) at moving reagents toward the transition state for reaction. Third, even though we find $3\nu_4$ to be less reactive than ν_3, we note that bending overtone and combination states in CH_4 have much higher degeneracies at a given level of vibrational excitation. Therefore, even though stretching states may be more reactive on a per-energy basis, the preponderance of excited bending states in a thermal distribution may result in bending states contributing significantly, or even dominating the reactivity of thermal distributions of methane molecules. Fourth, the data suggest that statistical theories are unreliable predictors of S_0 for individual states. Finally, differences in the reactivity of stretching and bending states point to complications in comparing the ensemble-averaged reactivity of nonthermal vibrational state populations in CH_4 beam experiments with corresponding thermally averaged quantities obtained from bulb measurements.

We gratefully acknowledge support by the National Science Foundation (CHE-0111446) and Tufts University.

[1] G. O. Sitz, Rep. Prog. Phys. **65**, 1165 (2002).
[2] D. C. Jacobs, J. Phys. Condens. Matter **7**, 1023 (1995).
[3] H. Hou, Y. Huang, S. J. Guiding, C. T. Rettner, D. J. Auerbach, and A. M. Wodtke, Science **284**, 1647 (1999).
[4] L. B. F. Juurlink, P. R. McCabe, R. R. Smith, C. L. DiCologero, and A. L. Utz, Phys. Rev. Lett. **83**, 868 (1999).
[5] A. C. Luntz, Science **302**, 70 (2003).
[6] J. H. Larsen and I. Chorkendorff, Surf. Sci. Rep. **35**, 165 (1999).
[7] M. B. Lee, Q. Y. Yang, and S. T. Ceyer, J. Chem. Phys. **87**, 2724 (1987).
[8] P. M. Holmblad, J. Wambach, and I. Chorkendorff, J. Chem. Phys. **102**, 8255 (1995).
[9] H. Yang and J. L. Whitten, J. Chem. Phys. **96**, 5529 (1992).
[10] A. C. Luntz, J. Chem. Phys. **102**, 8264 (1995).
[11] A. P. J. Jansen and H. Burghgraef, Surf. Sci. **344**, 149 (1995).
[12] P. Kratzer, B. Hammer, and J. K. Nørskov, J. Chem. Phys. **105**, 5595 (1996).
[13] J. D. Beckerle, A. D. Johnson, Q. Y. Yang, and S. T. Ceyer, J. Chem. Phys. **91**, 5756 (1989).
[14] R. Milot and A. P. J. Jansen, Phys. Rev. B **61**, 15 657 (2000).
[15] H. L. Abbott, A. Bukoski, D. F. Kavulak, and I. Harrison, J. Chem. Phys. **119**, 6407 (2003).
[16] A. Bukoski, D. Blumling, and I. Harrison, J. Chem. Phys. **118**, 843 (2003).
[17] E. Venuti, L. Halonen, and R. G. Della Valle, J. Chem. Phys. **110**, 7339 (1999).
[18] R. R. Smith, D. R. Killelea, D. F. DelSesto, and A. L. Utz, Science **304**, 992 (2004).
[19] P. R. McCabe, L. B. F. Juurlink, and A. L. Utz, Rev. Sci. Instrum. **71**, 42 (2000).
[20] L. S. Rothman *et al.*, J. Quant. Spectrosc. Radiat. Transfer **60**, 665 (1998).
[21] L. B. F. Juurlink, R. R. Smith, and A. L. Utz, J. Phys. Chem. B **104**, 3327 (2000).
[22] A. C. Luntz, J. Chem. Phys. **113**, 6901 (2000).
[23] H. A. Michelsen, C. T. Rettner, D. J. Auerbach, and R. N. Zare, J. Chem. Phys. **98**, 8294 (1993).
[24] M. P. Schmid, P. Maroni, R. D. Beck, and T. R. Rizzo, J. Chem. Phys. **117**, 8603 (2002).
[25] R. D. Beck, P. Maroni, D. C. Papageorgopoulos, T. T. Dang, M. P. Schmid, and T. R. Rizzo, Science **302**, 98 (2003).
[26] J. C. Polanyi, Acc. Chem. Res. **5**, 161 (1972).
[27] D. K. Bronnikov, D. V. Kalinin, V. D. Rusanov, Y. G. Filimonov, Y. G. Selivanov, and J. C. Hilico, J. Quant. Spectrosc. Radiat. Transfer **60**, 1053 (1998).